Int. J. Heat Mass Transfer. Vol. 36, No. 17, pp. 4181–4191, 1993
Printed in Great Britain

0017–9310/93 $6.00+0.00

A general analytical approach toward the thermal conductivity of porous media†

T. H. BAUER

Reactor Engineering Division, Argonne National Laboratory, 9700 South Cass Avenue, Argonne, IL 60439, U.S.A.

(*Received* 26 *January* 1993 *and in final form* 10 *May* 1993)

Abstract—A general analytical approach to the thermal conductivity of porous media is developed which leads to theoretically sound expressions having a wide range of applicability and easily fitted to available empirical data. Specifically, practical expressions are derived for pore distributions of any concentration, randomly oriented pores of arbitrary shape, pores of any conductivity, radiant heat transfer within pores, and fibrous media. Most results transfer freely to electrical conductivity or any other general area where Laplace's equation applies. Fundamental limitations of the approach restrict its use to random pore distributions and heat transfer through the continuous medium by conduction. Examples are chosen from selected problem areas of current interest, spanning a wide range of pore types, volume fractions, and conductivities.

INTRODUCTION

THIS PAPER revisits the very old analytical question of the alteration of a medium's thermal conductivity by a random distribution of pores. Fundamentally, the theoretical problem is to account for the microscopic distortion of the temperature field in the neighborhood of an individual pore and consistently calculate its influence on macroscopic temperature gradients. Applications to the wide variety of heterogeneous materials of current interest to engineering and the physical sciences are almost endless. In spite of the 'classical' nature of this problem, it may be surprising to note that there still remains a practical need for generally applicable, theoretically sound expressions for porous medium conductivity that can be applied over a wide range of pore composition, shapes, and concentrations.

In fact, obtaining theoretical assessments for practical problems can often be quite frustrating. Most historical and current reported work on the subject may be categorized as (1) highly application-specific empirical fits to data, (2) idealized microscopic treatments, or (3) macroscopic lumped-parameter engineering approaches. Application-specific work is too narrow in scope to be generally useful. Consequently, results from idealized microscopic treatments, dating back to pioneering efforts of Maxwell [1] are often employed to meet more general needs. While this original approach does account for the microscopic distortion of the temperature field, its use is usually restricted to dilute concentrations of regularly shaped pores [1–3]. In one case, however, Bruggeman [4] succeeded in generalizing Maxwell's spherical pore result to high concentrations. Alternative 'lumped parameter' macroscopic engineering approaches account for general mixtures of materials of any concentration [5] but are often grossly in error microscopically in the neighborhood of an individual pore.

Motivated by practical need, this paper proposes a general approach to thermal conduction in porous media intended for a wide range of applicability, suitable for purposes of design and analysis, and useful for both interpolation and extrapolation of experimental data. The approach is to generalize Maxwell's 'classical' theoretical result for dilute distributions of spherical pores [1] to pores of any shape and concentration. Bruggeman's earlier results for spherical pores [4] are included as a special case. The fundamental advance is the use of randomness, uniformity, and symmetry assumptions in key places to enable tractable solutions of potentially highly complex problems. Randomness of pore spatial distribution permits development of useful bounding and constraining relationships and allows results derived for dilute pore distributions to be generalized to all concentrations. Random pore orientation allows spherical symmetry to simplify the problem and reduce the effect of general pore shape to a 'shape factor' parameter, which may be determined empirically. The resulting empirical expressions for thermal conductivity are useful for any pore composition, shape, size, or concentration. To illustrate further extension of general methods, we include radiant heat transfer within pores. We also extend results to encompass fibers, which are modeled as macroscopically long cylindrical pores. Empirical fits are made in a few selected problem areas that illustrate a wide range of usefulness.

† Work performed under the auspices of the U.S. Department of Energy. Supported under Contract W-31-109-Eng-38.

NOMENCLATURE

A	dimensionless multiplier relating conductivity change to porosity
$A_{1,1}$	dimensionless multiplier appropriate to heat flow parallel, perpendicular to long fibers
B	constant determining temperature field inside a pore
C	multiplier of the dipole temperature field perturbation
e	emissivity of the inside surface of a transparent pore
K	thermal conductivity
K_e	effective thermal conductivity of the porous medium
K_p	thermal conductivity of the pore material
K_0	thermal conductivity of the unperturbed continuous medium
L	length of a long fiber
n	number of pores per unit volume
n	index of refraction of a transparent pore
P	porosity, $nV_p = (V - V_0)/V$
R	volumetric radius of a single pore
$R_{1,2}$	radius surrounding pore where temperature (1) or heat flux (2) is continuous
T	temperature
T_{inside}	temperature field inside a pore
$T_{outside}$	temperature field outside a pore
V	total volume of the porous medium
V_p	volume of an individual pore
V_0	total volume of the unperturbed continuous medium.

Greek symbols

α	ratio of K_p/K_0
ε	shape factor of a randomly oriented pore
$\varepsilon_{1,2}$	pore shape factors defined by $R_{1,2}/R$
σ	Stefan–Boltzmann constant.

PROBLEM DEFINITION

Formally, the analytical problem is to account for the effect of randomly distributed pores or inclusions on the solution of Laplace's heat conduction equation and to express the result as an altered 'effective' thermal conductivity through an equivalent 'homogenized' medium. This, of course, only makes physical sense to problems where macroscopic length scales are much larger than individual pores. Also, our attention is focused on heat transfer by conduction. Radiative heat transfer will be included only when it occurs inside the pores themselves. Convective heat transfer is not considered at all. While discussion in this paper is couched in the language of heat transfer, it is evident that most results transfer freely to electrical conductivity, or any other general area where Laplace's equation applies.

Our concept of 'porous medium' is intended to be very general and encompass any heterogeneous material consisting of identifiable continuous and randomly-distributed discrete phases. In all cases, the discrete phases are 'pores', regardless of which phase has the higher conductivity. For example, non-conducting 'holes' distributed within a conducting solid is a familiar example of a porous medium with the holes as pores and the solid as the continuous medium. Alternatively, solid debris within a gas or liquid would also be considered a porous medium with the solid debris as pores and the fluid as continuous medium. The porosity, P, is defined as the net volume fraction of the material occupied by pores. For pores of given composition and shape, our objective is to determine an effective macroscopic thermal conductivity as a function of P.

We define 'microscopic' and 'macroscopic' length scales as being 'the same as' or 'much larger than' the dimension of individual pores. Porosity, P, is calculated microscopically as the product nV_p, where n is a pore number density and V_p is an average pore volume. P is also calculated macroscopically as $(V - V_0)/V$ where V_0 is the volume of the continuous medium and V is the total volume, including pores.

BOUNDING MODEL AND CONSTRAINT

Certain macroscopic physical properties of a porous medium have a quite simple porosity dependence. For instance, material density turns out to be simply the average of the pore and continuous material densities weighted by the factors P and $1 - P$ respectively. A net swelling of the continuous medium, V/V_0 brought about by the addition of pore volume is calculated by $1/(1 - P)$.

While the porosity dependence of thermal conductivity is in general more complex, one simple but important bounding model closely follows the example of density. Let K_0 and K_p be the thermal conductivities of the continuous medium and pore material respectively, and K_e be the combined effective macroscopic conductivity. In a thin slice cut perpendicular to an assumed direction of macroscopic heat flow, a fraction, $1 - P$, of the area will conduct heat in proportion to thermal conductivity K_0, and the remaining fraction, P, of the area will conduct heat in proportion to thermal conductivity K_p. If this thin slice is placed in a uniform temperature gradient normal to the axial slice, K_e is given by an average of K_0 and K_p weighted by $1 - P$ and P respectively:

$$K_e|_{slice} = K_0(1 - P) + K_p P. \quad (1)$$

The analysis changes significantly, however, when extending the result of equation (1) to macroscopic thicknesses. In general, if a number of axial slices are stacked together each with randomly situated pores, the macroscopic heat flux appears uniform and normal to the axial slices, but the microscopic temperature gradient (and hence the direction of heat flow) in the vicinity of an individual pore is neither uniform nor normal to the axial slice. For instance, if the pores are non-conducting ($K_p = 0$), it is evident that heat must flow around each pore, and if pore locations change randomly from slice to slice, the truth path length for heat flowing through the medium must exceed the nominal macroscopic thickness of the slices. Because of this increased microscopic path length, the effective thermal conductivity will be less than implied by equation (1). In fact, as long as K_p differs significantly from K_0, heat flow traversing a number of axial slices deviates from normal either by systematically bending away from pores if $K_p < K_0$, or bending toward pores if $K_p > K_0$. In either case, if pores are randomly situated from slice to slice, the true path length for heat flow necessarily exceeds the nominal thickness of the material, and equation (1) overestimates effective thermal conductivity by the ratio of microscopic (actual) to macroscopic (nominal) path length. However, in the limiting case where $K_p \to K_0$ microscopic heat flow becomes normal to the slices, and equation (1) becomes exact. Equation (2) summarizes these considerations for correction factor K_e/K_0.

$$K_e/K_0 \leqslant 1-(1-K_p/K_0)P$$

and

$$\langle \cos\theta \rangle = \frac{K_e}{K_0(1-P)+K_pP}. \qquad (2)$$

In equation (2), equality holds in the limit $K_p \to K_0$, and $\langle \cos\theta \rangle$ refers to the average cosine of the angle between microscopic and macroscopic heat flow. These results are valid wherever pore distributions are random and represent general constraints and limits against which more detailed models and empirical relations may be tested.

It is useful at this point to comment on lumped parameter approaches to thermal conductivity of heterogeneous media. Such approaches envision a unit cell made up of a representative distribution of constituents connected by a minimal number of lumped 'series' and/or 'parallel' conduction paths. A macroscopic conductivity is then evaluated by combining these conductors into a single equivalent. Lumped parameter models are most useful in describing macroscopic situations where conduction paths are well defined and appropriate conductors can be realistically chosen on the basis of engineering judgement. For example, the widely used lumped parameter formalism developed by Kampf and Karsten [5] computes conductors assuming all heat flow in the problem is along the direction of macroscopic heat flow. However, our analysis leading to equation (2) indicates that, microscopically, this key heat flow assumption holds true only for very thin slices of material or in the limit $K_p \to K_0$. Because microscopic conduction paths where $K_p \neq K_0$ are in general complex, we conclude that lumped parameter models, such as ref. [5], will fall short (or at least be very difficult to implement) in analyses where temperature gradients and heat flow bend significantly in the neighborhood of individual pores.

GENERAL THEORY

For a more general treatment of conductivity we proceed toward a solution of Laplace's heat conduction equation in a porous medium that accounts for local distortion of the temperature profile as well as global amounts of material. At the microscopic level in the neighborhood of an individual pore, the longest-ranged temperature field perturbation induced is that of a 'dipole' heat source. It will be shown that modification of the material's thermal conductivity depends principally on the strength and concentration of such pore-centered dipole heat sources.

With considerable generality the perturbation of a uniform, unit temperature gradient by a distribution of identical pores in an otherwise uniform medium may be described by the equation:

$$T(r) = z + \int d^3r' n(r') \left[C \frac{z-z'}{|r-r'|^3} + \text{terms of order } \frac{(z-z')^2}{|r-r'|^4} \right]. \qquad (3)$$

$T(r)$ is the temperature at the point in space, $r = (x, y, z)$, in the uniform medium. Pores themselves are centered at space points, r', with a number density, $n(r')$. The applied unit temperature gradient is in the z direction.

Equation (3) is a particular solution to Laplace's equation, $\nabla^2 T(r) = 0$, in the uniform medium which meets the required boundary condition of a unit, uniform temperature gradient far away from all pores. The first term on the right hand side indicates the unperturbed unit temperature gradient. The additional terms represent a multipole expansion of temperature field perturbations centered at pore locations. The first perturbative dipole term, shown with the multiplier, C (dimension of volume), has both the longest range and the simplest angular dependence relative to the z axis. The additional 'higher order' perturbative terms indicated (symbolically) fall off more rapidly with distance and have more complex angular dependence. The coefficient, C, as well as coefficients of higher order perturbative terms, are determined on the basis of continuity of temperature and heat flux at the pore boundary surface.

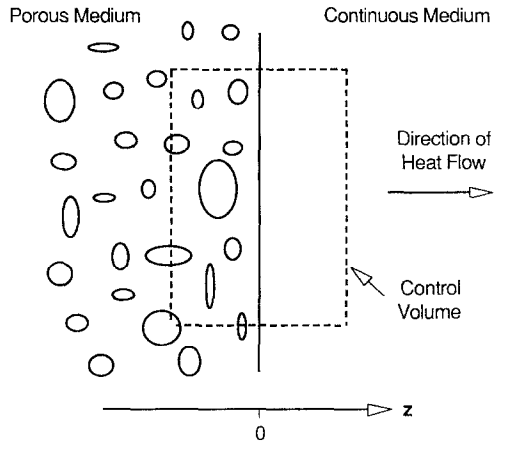

FIG. 1. Side view of a cylindrical control volume spanning the boundary between the porous and continuous media.

As long as $n(r')$ is a smooth function that is macroscopically slowly varying, it is useful to 'homogenize' the temperature field in the medium by formally extending the range of validity of equation (3) to include all space, even regions actually occupied by pores and singular regions where $r = r'$. In so doing, the Laplacian operating on the homogenized $T(r)$ is no longer identically zero but can be shown to be:

$$\nabla^2 T(r) = 4\pi C \frac{\partial n(r)}{\partial z} + \text{terms of order } \frac{\partial^2 n(r)}{\partial z^2} \quad \text{(homogenized temperature field)} \tag{4}$$

(Obtaining the equation (4) result makes use of the identity substitution: $-\partial(1/|r-r'|)/\partial z' = (z-z')/|r-r'|^3$ in equation (3) followed by an integration by parts with respect to z'. The Laplacian operation: $\nabla^2(1/|r-r'|) = -4\pi\delta(r-r')$ extracts the result shown.) With equation (4) we have mathematically extracted a multipole expansion of distributed pore-centered heat sources that would lead to the temperature field perturbations described in equation (3). The first such heat source on the right hand side, proportional to the gradient of the pore number density, represents each pore as a dipole heat source of strength proportional to $4\pi C$. The remaining terms, proportional to higher order spatial derivatives of the number density, represent higher-order multipole sources associated with each pore. We will now show that our desired modification of the medium's thermal conductivity is directly determined by these pore-centered heat sources.

Assume a semi-infinite slab of porous material in which pores are distributed uniformly in the x–y plane with a boundary located at $z = 0$ such that pore number density is n when $z < 0$, but 0 when $z > 0$. Figure 1 shows a selected cylindrical control volume placed within this configuration with axis parallel to the z-axis with one face located at $z < 0$ in the porous medium and the other at $z > 0$ in the continuous medium. For $z \gg 0$, a unit temperature gradient exists in the z-direction that is uniform over the x–y plane. Integrating both sides of equation (4) over an arbitrary control volume and applying the Gauss divergence theorem to the left hand side yields:

$$\oint \mathrm{d}S \cdot \nabla T(r) = \int \mathrm{d}V \left[4\pi C \frac{\partial n(r)}{\partial z} + \text{terms of order } \frac{\partial^2 n(r)}{\partial z^2} \right]. \tag{5}$$

Applying equation (5) to the configuration and control volume of Fig. 1, the left hand side yields the area of the control volume face times the difference in temperature gradient between the porous and continuous medium. Recognizing that the integrand contains only derivatives with respect to z, the right hand side yields the area of the control volume face times the quantity, $4\pi nC$. Importantly, only the dipole term on the right hand side survives this integration because derivatives of the number density are 0 on both sides of the $z = 0$ boundary. We are thus led to the very general result that the presence of pores alters the temperature gradient in the homogenized porous medium by a factor, $1 + 4\pi nC$.

Heat flux in the homogenized medium is given by conductivity times temperature gradient. Since heat flux is continuous in the z direction, the ratio of porous-to-continuous medium thermal conductivity equals the ratio of continuous-to-porous medium temperature gradient, or:

$$K_e/K_0 = 1/(1 + 4\pi nC). \tag{6}$$

Equation (6) is our fundamental expression describing the alteration of a medium's conductivity, and the determination of C, the dipole heat source generated by individual pores, will be the starting point and focus of subsequent analyses.

DILUTE PORE LIMIT

Evaluation of the dipole heat source C and equation (6) is much simplified in the limit of dilute pore concentrations, as defined by $4\pi nC \ll 1$. In this limit, temperature perturbations produced by individual pores interfere minimally with one another, and determination of C simplifies to a 'unit cell' type calculation of the perturbation of a unit temperature gradient by a single pore placed in a uniform medium. Dimensional considerations also imply that the pore size, itself, provides the only length scale, where C, having the dimension of volume, is necessarily proportional to the pore volume, V_p. Recalling that $nV_p = P$, we may write:

$$4\pi nC = A(K_p/K_0)P \quad \text{(dilute pore limit)} \tag{7}$$

where A is a dimensionless quantity depending on pore shape and the ratio of pore to continuous medium conductivities. To leading order in $4\pi nC$, equation (6) may also be written:

$$K_e/K_0 = 1 - A(K_p/K_0)P \quad \text{(dilute pore limit)}. \quad (8)$$

Derivations of A for pore-types of interest will be given subsequently. General thermal conductivity bounds implied by equation (2) apply also to equation (8) and impose important limits on the multiplier, A. As a function of $\alpha \equiv K_p/K_0$, $A(\alpha)$ must be greater than or equal to $1-\alpha$ for all $\alpha \geq 0$ with equality in the limit $\alpha \to 1$. Applying these constraints to non-conducting pores, for example, implies that A must be a constant greater than 1.

GENERALIZATION TO ALL PORE CONCENTRATIONS

Generalizing results to all pore concentrations is potentially very complex if pores are close enough together that temperature perturbations interfere. However, our approach here is to extend the utility of the expressions derived above for the dilute pore limit to all pore concentrations through a sequence of 'dilute' analyses. The key assumption is that temperature field perturbations produced by random pore distributions may be smoothed and averaged even down to a microscopic level. We note that extending a smoothing assumption down to microscopic length scales is only plausible for random distributions. In this picture, the smoothed and averaged influence of neighboring pores is included in the equivalent uniform medium in which each individual pore is embedded. Conceptually, pore volume can be added to the medium in small dilute increments so that pores included in each increment see a uniform medium that includes effects of previously added porosity and where each increment further modifies the equivalent thermal conductivity in accord with equation (8).

Mathematically, starting from the pure conducting medium of volume, V_0, and conductivity, K_0, we incrementally add randomly distributed pore volume, dV. At each step we have a new total volume, V, and effective thermal conductivity, K. From equation (8), the incremental change in thermal conductivity, dK, is given by:

$$\frac{dK}{K} = -A(K_p/K)\frac{dV}{V} \quad (9)$$

where the incremental 'P' of equation (8) has been replaced by dV/V. In equation (9), the function, A, takes on the role of a 'kernel' which generates particular solutions. Equation (9) may be integrated by separating the variables, K and V, provided that the functional dependence of $A(K_p/K)$ on continuous medium conductivity, K, is known. The range required for K would generally include values between K_0 and K_p. Equation (9) can then be the starting point for practical analysis to determine K as a function of V.

Similar approaches for extending dilute system results to higher concentrations have been published previously. As mentioned earlier, Bruggeman [4] generalized results for spherical pores originally obtained by Maxwell [1] to all pore concentrations. In the context of viscosity of dispersed media, Roscoe [6] similarly generalized to all concentrations a result obtained by Einstein [7] for low concentrations.

DISTRIBUTIONS OF PORE TYPES AND SIZES

Although we have so far assumed a distribution of identical pores, analyses are general enough to be useful in situations involving multiple pore types and sizes. In fact, provided amplitudes C and A are appropriately averaged, equations (3)–(8) are equally appropriate for a distribution of pore sizes, shapes and contents if such distributions are also uniform in space. The amplitude C becomes an average weighted by each pore type's number density, while the amplitude A becomes an average weighted by each type's porosity contribution. This averaging scheme for A accounts for the fact that A is a dimensionless multiplier depending only on pore shape and contents. (Note that A can also depend on pore size implicitly through these other variables, as described in an example below.)

However, some ambiguity arises in generalizing solutions of equation (9) to multiple pore types, and results may depend on the order in which pore types are averaged and integrated. While results in the dilute pore limit described by equation (8) are unique, they are not necessarily so at higher pore concentrations where temperature field perturbations from pores overlap. For example, averaging A over various pore types prior to integrating equation (9) yields one answer. However, different answers may be obtained if the integration to the same final configuration is performed on one pore type at a time, depending on the order of integration. In fact, it may be proven mathematically that the formal generalization of equation (9) to multiple pore types ($dK/K = -A_1 dV_1/V - A_2/V - A_3\, dV_3/V - \ldots$) does not yield a unique solution for $K(V_1, V_2, V_3, \ldots)$ unless the As are all the same. Formally, there are many possible solutions for K which depend on the particular path of integration. This mathematical reality reflects the fact that, when temperature field perturbations from pores overlap, the order in which contributions from different pore types are averaged and/or added requires, in effect, an additional physical assumption. Thus, where multiple pore types are present, the preferred order of integration is the one which makes the most physical sense. Furthermore, if multiple possibilities are present, the range of physically reasonable alternatives provide an uncertainty estimate to this present modeling approach.

For example, if a known fraction of originally empty porosity is backfilled with material of conductivity close to that of the continuous medium, it makes physical sense to first add in the minimal heat flow perturbations from the backfilled pores and add the larger heat flow perturbations from the remaining

empty pores later on. As a second example, if there is a wide range of pore size, it also makes the most physical sense to add pore volume in a sequence of increasing pore size. We note that pore size can enter into solutions of equation (9) *implicitly* through potential dependence of pore shape and content on size (as will be illustrated later, when radiant heat transfer inside pores is considered).

Although examples in the remainder of this paper will be restricted to single pore types, practical examples involving multiple pore types have been developed and will appear in future publications.

'UNIT CELL' ANALYSIS FOR RANDOMLY ORIENTED PORES

In this section we evaluate the 'unit cell' dipole heat source generated by single pores perturbing a uniform unit temperature gradient. Results of these analyses will determine the dimensionless multiplier, A, appropriate to all pore concentrations via solutions of the differential equation (9). Pores are assumed to contain conducting material, but radiant heat transfer within pores will also be included as an additional option. A special case of macroscopically long cylindrical pores is introduced to model fibers in a fibrous medium.

Results presented emphasize randomly oriented pores. While formal solutions to the unit cell heat transfer problem exist for pores of any shape and content, important simplification results when pores are randomly oriented. In this case, the effect of pore shape is plausibly accounted for as a pore 'shape factor' parameter contained within rather simple universal expressions. When an option for evaluating shape factors empirically is included, these expressions become useful in a very wide range of application.

A. *Spherical pores*

Spherical pores containing conducting material provide the simplest 'textbook' example [8]. The temperature field in the vicinity of a single spherical pore perturbing a uniform unit temperature gradient in the z direction may be written as:

$$T_{\text{outside}} = z + C\frac{z}{r^3}$$

$$T_{\text{inside}} = Bz. \tag{10}$$

The coordinate system is pore-centered. The expression for T_{outside}, to be applied outside the pore, is meant to be consistent with equation (3), including the dipole multiplier, C. Because of spherical symmetry only the 'dipole' contribution is present. The expression for T_{inside} is a matching solution to Laplace's equation that is regular at $r = 0$ to be applied inside the pore. The pore radius is R, and the thermal conductivities inside and outside the pore are K_p and K respectively. Parameters B and C from equation (10) (and A from equation (7)) may be determined by imposing continuity of temperature, $T_{\text{outside}} = T_{\text{inside}}$, and heat flux, $K\hat{c}T_{\text{outside}}/\hat{c}r = K_p\hat{c}T_{\text{inside}}/\hat{c}r$, at the pore boundary surface, $r = R$:

$$B = 3\frac{K}{K_p + 2K}; \quad C = \frac{K - K_p}{K_p + 2K}R^3;$$

and

$$A(K_p/K) = 3\frac{1 - K_p/K}{2 + K_p/K}. \tag{11}$$

Substituting the equation (11) expression for A into equation (8) replicates the classical conductivity correction obtained by Maxwell [1] in the dilute pore limit. As anticipated, the equation (11) expression for $A(K_p/K)$ also complies with the general constraints that $A(\alpha)$ must be greater than or equal to $1 - \alpha$ for all $\alpha \geqslant 0$ with equality applying in the limit $\alpha \to 1$. In particular, for non-conducting spherical pores: $A(0) = 3/2$.

B. *Randomly oriented pores of arbitrary shape*

Provided that they are randomly oriented, pores of arbitrary shape perturb a uniform temperature gradient similarly to pores which are purely spherical. Randomizing pore orientations basically eliminates any directional preference to the angular dependence of temperature field perturbations, apart from the original direction of heat flow. The upshot is that, when pore orientation is averaged, the general form of expressions for T_{outside} and T_{inside} must simply average-out to the dipole expressions given in equation (10). As with spherical pores, our approach here will be to evaluate equation (10) multipliers B and C by applying temperature and heat flux continuity across averaged boundary surfaces. Symmetry implies that such boundary surfaces must be spherical. However, we account for a generalized pore shape by recognizing that the radii at which heat flux and temperature continuity apply may be different. Indeed, temperature and heat flux at a spherical pore boundary are sensitive to different powers of radius: so, in averaging over non-spherical pores, different surface radii are quite plausible.

We proceed in an empirical fashion by assuming 'inside' to 'outside' continuity of temperature and that radial heat flux occur at radial locations, to be determined. We define a radius, R_1, to be the value of r where $T_{\text{outside}} = T_{\text{inside}}$. Likewise, we define a radius, R_2, to be the value of r when $K\hat{c}T_{\text{outside}}/\hat{c}r = K_p\hat{c}T_{\text{inside}}/\hat{c}r$. R_1 and R_2 are to be compared with a volumetric radius, R, defined by: $V_p = 4\pi R^3/3$. 'Shape factors', $\varepsilon_1 = R_1^3/R^3$ and $\varepsilon_2 = R_2^3/R^3$, are then dimensionless parameters which quantify the deviation from spherical pores. Following these definitions, B, C and the dimensionless multiplier, A, may be evaluated in terms of R, ε_1, and ε_2. The solution for A yields:

$$A(K_p/K) = 3\frac{1 - K_p/K}{2/\varepsilon_2 + (K_p/K)/\varepsilon_1}. \tag{12}$$

However, in light of the bounding constraints of equation (2) the two shape factors appearing in equation (12) are not really independent. Imposing, $A(\alpha) \geqslant 1-\alpha$ and $A(\alpha) = 1-\alpha$ as $\alpha \to 1$, implies $1/\varepsilon_1 + 2/\varepsilon_2 = 3$ and $\varepsilon_2 > 2/3$. Defining one independent shape factor, $\varepsilon = \varepsilon_2$, equation (12) becomes:

$$A(K_p/K) = 3\frac{1-K_p/K}{2/\varepsilon + (3-2/\varepsilon)K_p/K}. \qquad (13)$$

From the standpoint of rigor, the orientation averaging procedure used in the preceding derivation is subject to some criticism. Specifically, results may not be exact in applications where pores are both highly irregular and also span a wide range of K_p/K. Rigorously, continuity across the pore boundary is required for each particular pore orientation, and averaging of the dipole temperature field perturbation over all orientations should be done afterward. While the symmetry and continuity arguments used in the development of equation (12) are quite correct, our approach tacitly assumes that averaged pore surface radii, R_1 and R_2, will be determined by pore geometry alone. Therefore, any explicit dependence of surface radii and shape factors on K_p/K will be neglected. Note that our assumption of 'geometrically dominated' surface radii is physically plausible (and correct, of course, in the spherical pore limit). Furthermore, application of equation (2) constraints assure overall K_p/K dependence of equation (13) will be consistent with fundamental principles. So, unless pore shape is extremely irregular, the neglected K_p/K dependence is likely to be weak. Our approach clearly has a practical advantage of avoiding potentially intractable analytical evaluations when pores are irregular, and succeeds in addressing effects of a general pore shape by a single parameter.

Equation (13) is thus proposed as the generalization of equation (11) to randomly oriented pores of any shape for use in the solution of equation (9). The effect of pore shape is described by a single unknown constant 'shape factor', ε, where $\varepsilon = 1$ for spheres and constrained to be $>2/3$. In practice, for distributions of irregularly shaped pores, it is quite convenient to regard ε as a constant to be determined empirically. Even if pores of various shapes are present, a single shape factor may be adequate depending on the relevant range of K_p/K. For instance, if pores are nonconducting, an average shape factor, ε_{avg}, represents the porosity-weighted average of individual shape factors, ε. On the other hand, if pores are highly conducting ($K_p/K \gg 1$), an average shape factor, ε_{avg}, represents a porosity-weighted averaging of the quantity, $\varepsilon/(3\varepsilon-2)$. Finally, if pore conductivities are such that $K_p \approx K$, consistency with equation (2) implies that A becomes nearly independent of ε.

C. *Radiative heat transfer within pores*

It is also possible for our present analyses to include heat transfer by radiation within pores. In situations where pore contents are transparent to radiation and the continuous medium is opaque, significant amounts of heat transfer by radiation can take place in pores at high absolute temperatures. Basically, the fundamental approach to effective conductivity outlined in equations (3)–(6), which requires conductive heat transfer outside of pore boundaries, is still valid. However, an additional radiative heat flux inside the pore will alter the dipole field perturbation produced by the pore (multiplier C) and hence change the effective conductivity of the porous medium.

The radiative heat flux emitted from the surface of a transparent pore may be quantified as $\sigma e n^2 T^4$, where σ is the Stefan–Boltzmann constant, e is pore surface emissivity, n is the transparent medium's index of refraction, and T is the absolute temperature at the pore surface. In general we may express pore surface temperature as $T+\mathrm{d}T$, where T is the pore average and $\mathrm{d}T$ describes an assumed small temperature variation around the pore surface ($\mathrm{d}T \ll T$) that averages to 0. In the case of a unit temperature gradient perturbed by spherical pore centered at the origin, the equation (10) expression for $T_{outside}$ implies that $\mathrm{d}T = (R + C/R^2)\cos\theta$, where θ is the polar angle with respect to the original direction of heat flow. Thus, for spherical pores, emitted heat flux around a pore surface may be approximately linearized to a term that is constant: $\sigma e n^2 T^4$, plus one which is varying:

$$4\sigma e n^2 T^3 \mathrm{d}T \quad \text{or} \quad 4\sigma e n^2 T^3 (R + C/R^2)\cos\theta.$$

The net radiative heat flux into the pore at any surface location is calculated on the basis of both emitted flux and interchange with other locations on the surface. In the case of the constant emitted heat flux term ($\sigma e n^2 T^4$), emission is exactly balanced by interchange, resulting in no net heat flux. However, the varying portion of the heat flux requires a more careful analysis. Interchange of homogeneously emitted radiation is proportional not only to total radiation emitted but also to geometrically determined 'radiation shape factors' [9] that account for orientation of the two surfaces and the distance between them. Significantly, it turns out for spherical surfaces that radiation shape factors between any two surface locations are the same. For the varying emitted heat flux term ($4\sigma e n^2 T^3 \mathrm{d}T$), uniform radiation shape factors imply that contributions deposited at any location by interchange will share the same angular dependence around the surface as $\mathrm{d}T$ and average to 0. Thus, for spherical pores we have the result that the net radiative heat flux into the pore is equal to the varying emitted heat flux into the pore, i.e. $4\sigma e n^2 T^3 (R + C/R^2)\cos\theta$.

Applying continuity of temperature and heat flux at the spherical pore boundary using equation (10) expressions for $T_{outside}$ and T_{inside} yields results for B, C, and A similar to equation (11). The principal change is the addition of an effective radiation term K_r to the pore conductivity K_p as it is used in equation (11):

$$K_p \rightarrow K_p + K_r, \quad \text{where } K_r = 4\sigma e n^2 T^3 R \quad \text{(spherical pores).} \tag{14}$$

To add a radiation contribution to pores of general shape, we adapt out earlier approach of applying spherically symmetric continuity conditions to a pore of average orientation. Recalling that R_1 is the radial location where, on average, $T_{outside} = T_{inside}$, the net radiative heat flux leaving the surface of an averaged pore becomes $4\sigma e n^2 T^3 (R_1 + C/R_1^2)\cos(\theta)$. Adding this heat flux to the others implicit in equation (10) and imposing heat flux continuity at radius, R_2 yields results similar to equations (12) and (13), provided that effective pore conductivity contains a radiation term similar to equation (14). Here, K_r reflects the dimension R_1. In terms of the pore shape factor ε and volumetric radius R, the radiative contribution to pore conductivity becomes:

$$K_r = 4\sigma e n^2 T^3 R(\varepsilon/(3\varepsilon - 2))^{1/3} \quad \text{(pores of general shape).} \tag{15}$$

Despite maintaining the general form of earlier results, the presence of radiation adds potentially significant temperature and pore-size dependence to the analysis. It was argued previously on the basis of dimensional analysis that the dimensionless parameter A should be independent of pore size. Including radiation adds new length scales that enter the problem implicitly in the guise of an additional conductivity, K_r that is proportional to both pore radius and the cube of absolute temperature. In accord with our previous discussion on distributions of pore shapes and sizes, this new dependence of A on pore size may be important when integrating equation (9).

D. *Fibers as cylindrical pores of infinite length*

We approach the thermal conductivity of a fibrous medium by modeling a fiber as a macroscopically long cylindrical pore. Not surprisingly, the effect of fibers on conductivity depends strongly on whether they are oriented parallel or perpendicular to macroscopic heat flow. Thus, we allow for a distribution of cylinder axis orientation with respect to the direction of macroscopic heat flow. In practice, the axial orientation of fibers can have either a preferred direction, preferred plane, or be random. Long fibers may also be bent or twisted over macroscopic distance scales.

In the simplest case, where the fiber axis is parallel to the direction of macroscopic heat flow, there is no local distortion of the temperature field. The reasoning leading to equation (1) applies, effective conductivity is given by a volume weighted average of K_0 and K_p, and the dimensionless multiplier, denoted $A_{\parallel}$, becomes $A_{\parallel} = 1 - K_p/K_0$.

On the other hand, where the fiber axis is perpendicular to macroscopic heat flow, the temperature field perturbation is more complex. In this case, we model the temperature field produced by a single long cylindrical pore as a uniform distribution of point pores extending for a length, L, along the y axis that perturbs a uniform unit temperature gradient along the z axis. In pore-centered cylindrical coordinates, radial distance from the cylinder, ρ is defined by $\rho^2 = x^2 + z^2$, and ϕ is the azimuthal angle formed by the radius vector and the z axis, such that $z = \rho\cos\phi$ and $x = \rho\sin\phi$. The temperature field outside the cylinder is determined by integrating equation (3) over pore locations along the y axis. Results for temperature fields both inside and outside the cylinder are shown in equation (16), retaining terms associated with the longest range dipole contributions. Equation (16) is clearly the analog of equation (10) for cylindrical pores, where the dipole strength C has been replaced by a dipole strength per unit length C/L.

$$T_{outside} = z + 2\frac{C}{L}\frac{z}{\rho^2} = \rho\cos\phi + 2\frac{C}{L}\frac{\cos\phi}{\rho}$$
$$T_{inside} = Bz = B\rho\cos\phi. \tag{16}$$

Following analysis techniques developed earlier, constants C and B are determined by applying continuity of temperature and heat flux at the cylinder boundary. Following the definition of equation (7), the dimensionless multiplier for this case, $A_{\perp}$, is defined for cylinders as $4\pi C/\pi R^2 L$. If the cylinder cross section is circular, both continuity conditions occur at the outer radius, R. If the cylinder is of general shape, the two continuity conditions for the randomly oriented cylinder occur at averaged radii R_1 and R_2, which may differ from an areal averaged radius R. However, in this case applying bounding constraints of equation (2) to the result forces $R_1 = R_2 = R$. Thus, no shape factor appears in the analysis of cylindrical pores provided the areal radius is used in all expressions. It follows that $C/L = (R^2/2)(1 - K_p/K_0)/(1 + K_p/K_0)$ and $A_{\perp} = 2(1 - K_p/K_0)/(1 + K_p/K_0)$. This expression for $A_{\perp}$ may be regarded as the cylindrical analog of the corresponding expression for spheres from equation (11).

If the fiber is generally oriented at an angle θ with respect to the macroscopic direction of heat flow, a multiplier, A, may be calculated as an appropriate average of the above cases of parallel and perpendicular orientation; i.e. $A_{\perp}\cos^2\theta + A_{\parallel}\sin^2\theta$. The general multiplier for a fibrous medium becomes:

$$A(K_p/K_0, \theta) = (1 - K_p/K_0) \times \left(\cos^2\theta + \sin^2\theta \frac{2}{1 + K_p/K_0}\right). \tag{17}$$

If fibers are randomly oriented, $\sin^2\theta = 2/3$ and $\cos^2\theta = 1/3$.

EXPRESSIONS FOR GENERAL APPLICATION AND SELECTED EXAMPLES

A. *General result for a single pore type*

As discussed earlier, the expression for $A(K_p/K)$ for single types of randomly oriented pores from equation

(13) is a result that is very useful in a wide range of practical applications. These applications can include multiple pore types where an averaged pore shape or content is appropriate. Equation (9) may be straightforwardly integrated by separation of variables, K and V, to yield:

$$\frac{K-K_p}{K_0-K_p}\left(\frac{K_0}{K}\right)^{1-(2/3\varepsilon)} = 1-P \quad \text{(single pore-type)} \tag{18}$$

where we have substituted $1-P$ for V_0/V, and take K_0 as the continuous medium conductivity. Equation (18) implicitly determines effective thermal conductivity, K, as a function of porosity, P for all values of K_p.

Because shapes of isolated pores in dilute systems may be different from pores in high-porosity systems where they are crowded together, shape factors may themselves depend on the total porosity. Some functional dependence of ε on P should be considered when fitting conductivity data. Note, however, that the shape factor should remain constant during the mathematical integration of equation (9) at a value appropriate to the final porosity at the end of the integration.

B. *Low-conductivity pores*

For the special case of non-conducting pores, $K_p = 0$, equation (18) simplifies to:

$$K/K_0 = (1-P)^{3\varepsilon/2} \quad \text{(non-conducting pores)} \tag{19}$$

providing the analytical form for application in the low pore-conductivity limit.

For a practical illustration emphasizing application in regions of high pore concentration, we apply equation (19) to a database consisting of electrical conductivity measurements of liquid foams. (The dependence of electrical conductivity on the amount of non-conducting porosity should be identical to that of thermal conductivity.) The data shown on Fig. 2, taken from ref. [10], shows measured porosity dependence of electrical conductivity for a variety of liquid foams, spanning a wide range of liquid electrical conductance and a porosity range of about 0.6 to 0.95. Note that measured porosity dependence seems little influenced by the absolute conductivity or any other feature of the particular liquid involved. The line drawn, showing an excellent fit to the data, is equation (19) with a constant value of $\varepsilon = 0.863$.

C. *Highly-conducting pores*

Solid–gas debris- or pebble-bed mixtures serve as a contrasting example where pore conductivity is high. Figure 3 shows thermal conductivity measurements from various debris bed sources compiled by Kuzay [11] plotted against the conductivity of the solid pore constituent. Conductivity ratios shown are relative to that of the gaseous continuous medium. Mixtures shown in Fig. 3 represent stationary compact beds of

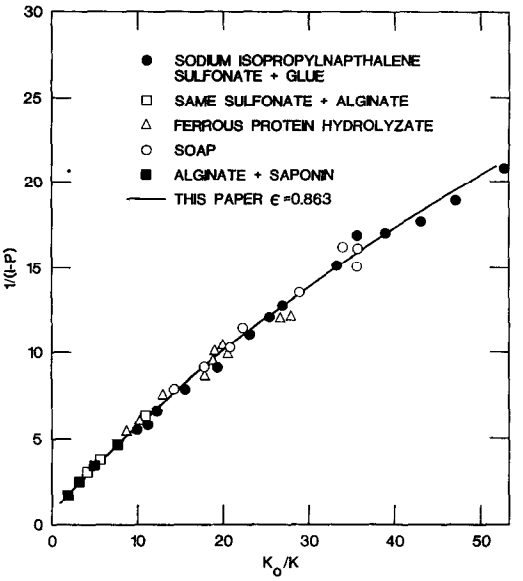

FIG. 2. Electrical conductivity vs density of various foams from ref. [10]. The curve shown is equation (19) with $\varepsilon = 0.863$.

uniform spherical solid 'pores' with porosity clustered around 0.6. The ratio of K_p/K_0 spans a wide range from around 1.8 to 60 000.

The prediction of equation (18) for spherical pores, $\varepsilon = 1$, requiring no free parameters, is seen to provide a good fit to the data over its entire range. (We note that this spherical pore limit of equation (18) was first derived by Bruggeman [4].) In the high conductivity limit where $K_p/K_0 \gg 1$, equation (18) simplifies to:

$$K/K_0 = (1-P)^{-(3\varepsilon/(3\varepsilon-2))} \quad \text{(highly-conducting pores)}. \tag{20}$$

For $P = 0.6$ and $\varepsilon = 1$, equation (20) implies a limiting conductivity ratio of 15.6, which is also in good agreement with the data shown on Fig. 3.

D. *Fibrous media*

In the case of a general fibrous medium, equation (9) is integrated using the equation (17) expression for $A(K_p/K_0, \theta)$ to yield:

$$\left(\frac{K-K_p}{K_0-K_p}\right) \times \left\{\frac{K+[(1-\sin^2\theta)/(1+\sin^2\theta)]K_p}{K_0+[(1-\sin^2\theta)/(1+\sin^2\theta)]K_p}\right\}^{-(\sin^2\theta/(1+\sin^2\theta))} = 1-P \quad \text{(fibrous medium)} \tag{21}$$

where $\sin^2\theta$ reflects the average orientation of fibers in the distribution relative to macroscopic heat flow. Because exact fiber orientation is often not known or difficult to engineer, $\sin^2\theta$ can plausibly serve as an adjustable parameter in data analysis. Figure 4 shows equation (21) calculations for K/K_p for a range of orientations in the highly-useful limit of high con-

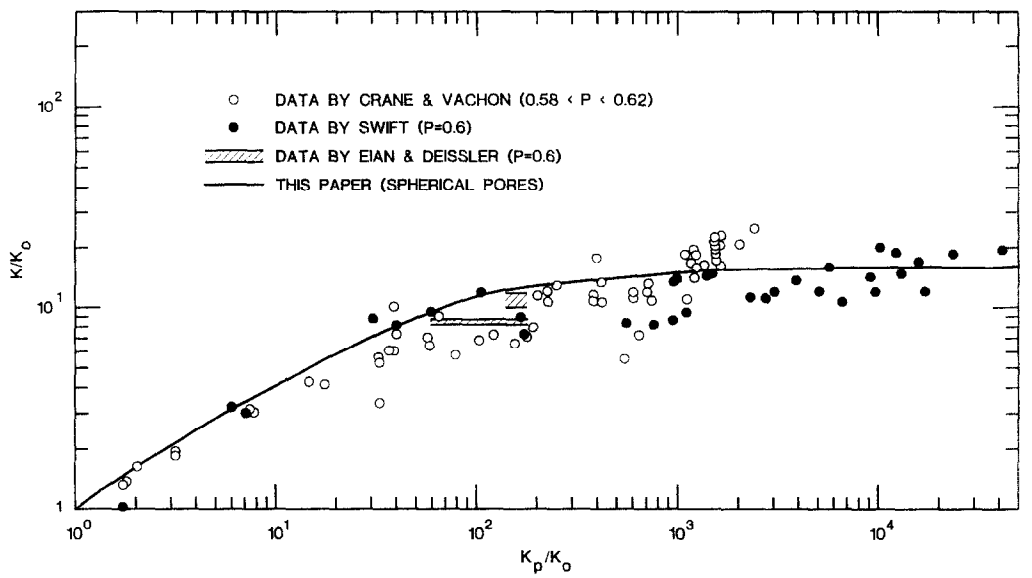

FIG. 3. Effective thermal conductivity of solid–gas mixtures as compiled by Kuzay [11]. Data are from packed spherical beds with porosity values around 0.6. Prediction of equation (18) with $\varepsilon = 1$ (no free parameters) is shown. This equation was first obtained by Bruggeman [4].

ductivity fibers placed in a low-conductivity medium, $K_p/K_0 \gg 1$. At the extremes, when $\sin^2\theta = 0$, K/K_p varies linearly between 0 and 1 as a function of porosity, but is identically 0 for all porosities, if $\sin^2\theta = 1$. These calculations illustrate an important role for fiber orientation as well as porosity, itself, in maintaining low conductivity across an insulating medium.

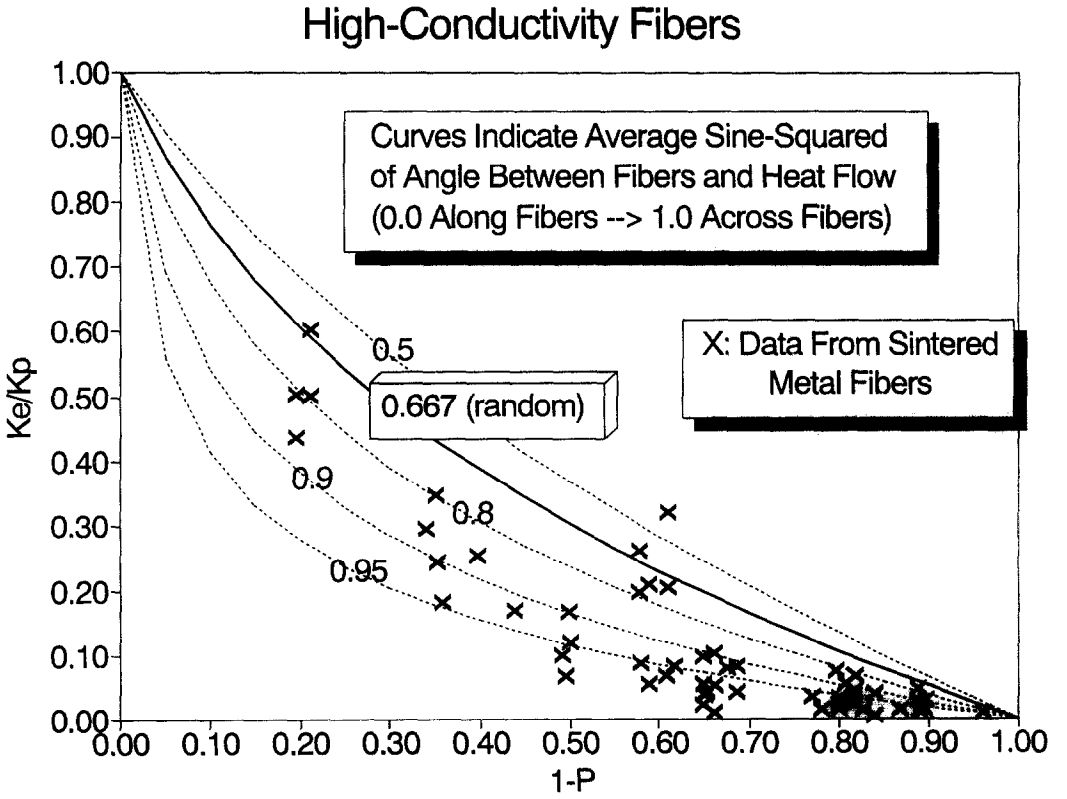

FIG. 4. Conductivity of a medium containing high-conductivity fibers with varying porosity and fiber orientation. Data are taken from ref. [12]. Curves are calculated from equation (21).

Figure 4 also includes conductivity data compiled in Mantle and Chang [12] for a variety of sintered metal fibers distributed across a low-conductivity continuous medium ($K_p/K_0 > 0.01$). As reported in ref. [12], fiber orientation was not always well known, but at least in some measurements direction of heat flow was nominally across fibers. While a single value of $\sin^2\theta$ does not seem to fit all the included data, there is a clear indication that the data is best fit by cases where $\sin^2\theta > 0.667$ or that heat flows preferentially across fibers. This preference for heat flow direction is more evident at low porosities than at high.

CONCLUSIONS

The principal conclusion drawn from this work is that the classical problem of the porosity dependence of thermal conductivity in porous media can be made analytically tractable under the assumptions that pore distributions are uniform and random. The randomness of the distribution is required to be of sufficient degree that the microscopic perturbations of the temperature field produced by representative samples can be smoothed and averaged. Limitations of the methods are generally benign, and analytical results are remarkably free of restriction. Application is appropriate to pore distributions of any concentration, any pore conductivity, and any pore shape (provided, of course, pore orientation is also random). Multiple pore sizes and types are also permitted. Simplicity and wide range of applicability of the present approach offers significant advance over previous treatments of the subject.

Application of the derived general expressions to practical problems is straightforward and very amenable to empirical fits. Typically, only one free parameter, the 'shape factor', requires empirical input if pores are of some irregular shape but are randomly oriented. Illustrative examples included pores of low and high thermal conductivity, a wide range of pore volume fractions, non-spherical pore shapes, and the use of adjustable parameters. Very reasonable fits to data were obtained. While single pore-types were used for these illustrations, practical expressions are readily generalized to distributions with multiple pore shapes, sizes and/or contents. Additional applications will appear in a future publication.

REFERENCES

1. J. C. Maxwell, *A Treatise on Electricity and Magnetism*, Vol. I (3rd Edn). Oxford University Press (1891), reprinted by Dover, New York (1954).
2. A. L. Loeb, Thermal conductivity: VIII, a theory of thermal conductivity of porous materials, *J. Am. Ceram. Soc.* **37**, 96–99 (1954).
3. A. Biancheria, The effect of porosity on thermal conductivity of ceramic bodies, *Trans. Am. Nucl. Soc.* **9**, 15 (1966).
4. D. A. G. Bruggeman, Calculation of different physical constants of heterogeneous substances I: dielectric constant and conductivity of media of isotropic substances, *Ann. Phys.*, Series 5 **24**, 636 (1935).
5. H. Kampf and G. Karsten, Effects of different types of void volumes on the radial temperature distribution of fuel pins, *Nucl. Appl. Technol.* **9**, 288–300 (1970).
6. R. Roscoe, The viscosity of suspensions of rigid spheres, *Br. J. Appl. Phys.* **3**, 267–269 (1952).
7. A. Einstein, New determination of molecular dimensions, *Ann. Phys.* **19**, 289–306 (1906); **34**, 591 (1911).
8. L. D. Landau and E. M. Lifshitz, *Fluid Mechanics*, p. 191. Pergamon Press (1959).
9. F. Kreith and M. S. Bohn, *Principals of Heat Transfer* (4th Edn), p. 457. Harper and Row, New York (1986).
10. N. O. Clark, The electrical conductivity of foam, *Trans. Faraday Soc.* **44**, 13–14 (1948); reported in J. J. Bikerman, *Foams*. Springer, Berlin (1973).
11. T. M. Kuzay, Effective thermal conductivity of porous solid–gas mixtures, ASME Winter Ann. Mtg., Paper 80-WA/HT-63, Chicago (1980).
12. W. J. Mantle and W. S. Chang, Effective thermal conductivity of sintered metal fibers, *J. Thermophys.* **5**, 545–549 (1991).